
SYNTHESIS AND PROPERTIES OF INORGANIC COMPOUNDS

Synthesis and Photocatalytic Properties of Low-Dimensional Cobalt-Doped Zinc Oxide with Different Crystal Shapes

V. N. Krasil'nikov, O. I. Gyrdasova, L. Yu. Buldakova, and M. Yu. Yanchenko

*Institute of Solid State Chemistry, Ural Branch, Russian Academy of Sciences,
Pervomaiskaya ul. 91, Yekaterinburg, 620041 Russia*

Received June 19, 2009

Abstract—The glycooxide complexes $Zn_{1-x}Co_x(HCOO)(HOCH_2CH_2O)_{1/2}$ and $Zn_{1-x}Co_x(OCH_2CH_2O)$ ($0 \leq x \leq 0.3$) have been synthesized by heating ethylene glycol solutions of zinc formate $Zn(HCOO)_2 \cdot 2H_2O$ or its mixtures with cobalt formate $Co(HCOO)_2 \cdot 2H_2O$. The crystals of these complexes have the shape of filaments (needles, bars) and distorted octahedra, respectively. A new method in which these complexes are used as the precursor is suggested for the synthesis of low-dimensional wurtzite-like $Zn_{1-x}Co_xO$. The shape of the precursor crystals is fully inherited by $Zn_{1-x}Co_xO$ resulting from their heat treatment. The $Zn_{1-x}Co_xO$ solid solutions show high photocatalytic activity in hydroquinone oxidation in aqueous solution under UV or blue light irradiation, and their activity increases as their cobalt content is increased.

DOI: 10.1134/S0036023611020136

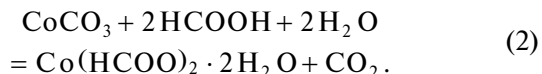
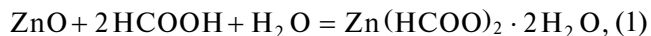
Zinc oxide belongs to the family of multifunctional wide-bandgap semiconductors, which have been the subject of extensive studies in recent years [1, 2]. Particular attention have been focused on the synthesis of micron- and nanometer-sized oxides consisting of quasi-one-dimensional (1D), extended particles (rods, needles, whiskers, filaments, tubes). It is anticipated that these oxides will possess new, better functional properties [3–5]. A very important appropriateness criterion for these methods is whether the morphology of the resulting oxide particles is controllable [6]. One of the currently central and most promising applications of zinc oxide is photocatalytic oxidation of organic compounds and disinfection of water and air [7–12]. The bandgap width of zinc oxide is 3.37 eV, so undoped zinc oxide is active only in the UV region of the spectrum. Its functional characteristics are modified by doping it with *d*- and *f*-elements, and this doping has afforded materials and devices with very interesting and valuable properties, including room-temperature ferromagnets, gas and optical sensors, phosphors, transistors, light-emitting diodes, and even catalysts for oxidation of toxic organic compounds [13–15]. However, the relevant literature deals mainly with oxidative photocatalysis on high-porosity and grained materials. There are only scarce data concerning the photocatalytic activity of zinc oxide consisting of extended particles [11–13], and we failed to find any photocatalytic data for zinc oxide doped with other transition elements. This prompted us to study the formation conditions for zinc oxide and $Zn_{1-x}Co_xO$ solid solutions as extended micron- and nanometer-sized particles and to test the photocatalytic activity of these materials in hydroquinone oxidation in water under UV and visible radiation.

In recent years, preparative nanochemistry has been increasingly using precursor techniques in the synthesis of quasi-1D oxides. The precursors employed in these techniques are metal carboxylates and glycoxides crystallizing as sticks or filaments whose length is tens or even hundreds of times larger than their diameter. On heating, these compounds turn into oxides, whose particles retain the shape of the precursor crystals [16–18]. In this study, fine ZnO and $Zn_{1-x}Co_xO$ powders consisting of extended particles were synthesized by the thermolysis of glycooxide complexes obtained by heat treatment of $Zn(HCOO)_2 \cdot 2H_2O +$ ethylene glycol and $(1 - x)Zn(HCOO)_2 \cdot 2H_2O + xCo(HCOO)_2 \cdot 2H_2O +$ ethylene glycol mixtures [19].

EXPERIMENTAL

The existing methods of synthesis of metal glycooxide complexes are based on hydrothermal treatment of alkoxides in ethylene glycol. The latter is taken in excess and serves both as the solvent and as a reactant [16–19]. The syntheses of the zinc glycooxide precursors for obtaining fine-particle zinc oxide included the following operations. $HOCH_2CH_2OH$ (analytical grade) was poured into four 150-mL heat-resistant glass beakers, 50 mL in each, and 2.5 g of zinc formate $Zn(HCOO)_2 \cdot 2H_2O$ was added into each beaker. Three of the resulting mixtures were heat-treated at 50, 100, and 150°C for 12 h with intermittent stirring. The fourth mixture was heated to 200°C under stirring and was held at this temperature for 1 h. The solid products were separated from the liquid phase by vacuum filtration, washed with absolute acetone, dried at 40°C for removing the acetone, and placed in weighing bottles

with ground-glass stoppers to rule out the effect of atmospheric moisture. The $(1-x)\text{Zn}(\text{HCOO})_2 \cdot 2\text{H}_2\text{O} + x\text{Co}(\text{HCOO})_2 \cdot 2\text{H}_2\text{O}$ mixtures, with x varied up to 0.3, were heat-treated in the same way. Zinc and cobalt formates were synthesized by reacting formic acid (analytical grade) with zinc oxide (special-purity grade) and cobalt carbonate (analytical grade), respectively:

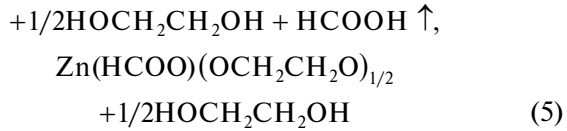
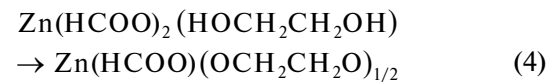
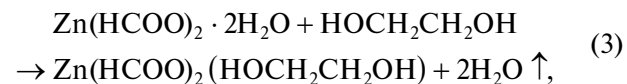


The phase composition of the precursors and their thermolysis products was determined by X-ray powder diffraction (DRON-2 diffractometer, $\text{Cu}K_\alpha$ radiation) and transmission light microscopy (POLAM S-112 polarizing microscope). Refractive indexes were measured using a set of standard immersion liquids. Thermo-gravimetric analysis was carried out on a Q-1500D thermoanalytical system in air at a heating rate of 10 K/min. The IR spectra of powders were recorded on a Spectrum-One spectrometer (PerkinElmer) in the 400–4000 cm^{-1} range. Particle shapes and sizes were determined by scanning electron microscopy (SEM) using a Tesla BS-301 instrument. The zinc and cobalt contents were determined by atomic absorption spectroscopy (PerkinElmer spectrometer, acetylene–air flame) and by inductively coupled plasma–atomic emission spectroscopy (JY-48 spectrometer). To determine the total carbon content, the sample to be analyzed (0.02–0.20 g) was covered with a CuO flux and was burned in flowing oxygen at 1200°C. In the quantification of free carbon, we made use of the fact that free carbon is inert toward the hydrofluoric acid + nitric acid mixture, as distinct from carbon bound to a metal. A 0.20-g sample was placed in a platinum bowl, HF (50 mL) and HNO_3 (special-purity grade, 1–2 mL) were added, and the mixture was heated on a stove until the complete dissolution of the solid. Next, the contents of the bowl were evaporated to wet salts, 20 mL of water was added, and the mixture was evaporated again. This evaporation–water addition procedure was repeated three times. The resulting solid was collected on an asbestos filter, washed with water until pH 7, and dried at 110–120°C. Its carbon content was determined as the amount of carbon dioxide resulting from the heating of the sample in flowing oxygen using a Metavak-CS express analyzer. The specific surface area of the thermolysis products of the glycoxide complexes was estimated by low-temperature nitrogen adsorption (BET method) on a TriStar 3000 automated analyzer (Micromeritics, United States). The solutions of hydroquinone (analytical grade, 0.01 mol/L), in 50-mL quartz beakers, were UV-irradiated using a BUF-15 lamp ($\lambda_{\max} = 253$ nm). Visible light irradiation was carried out using a blue luminescent lamp ($\lambda_{\max} = 440$ –460 nm). Current–voltage measurements in the solutions were performed with a PU-1 polarograph at a potential scan rate of 0.030 V/s.

Anodic voltammograms were recorded in the 0.0–1.0 V potential range; cathodic voltammograms, between 1.0 and –0.5 V. The indicator electrode was a cylindrical glassy carbon electrode with a working surface area of 0.44 cm^2 . The reference and auxiliary electrodes were saturated Ag/AgCl electrodes (EVL-1M3). The supporting electrolyte was 0.03 M sodium sulfate (special-purity grade).

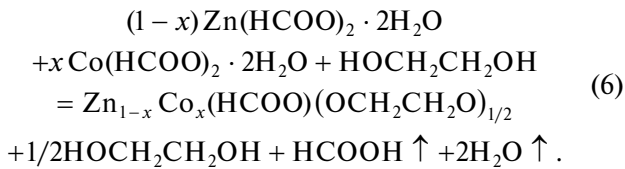
RESULTS AND DISCUSSION

According to the phase, elemental, and physicochemical analyses of the heat-treatment products of $\text{Zn}(\text{HCOO})_2 \cdot 2\text{H}_2\text{O}$ mixed with ethylene glycol, the interaction between the components takes place in three steps according to the following chemical equations:

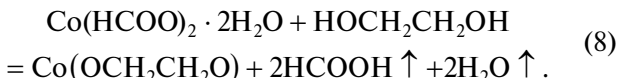
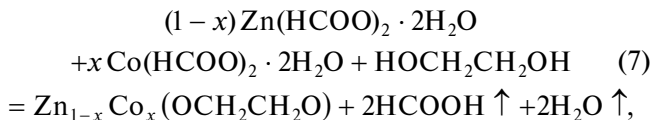


As is clear from chemical equation (3), the first step of this interaction, which occurs at ~50°C, yields the solvate $\text{Zn}(\text{HCOO})_2(\text{HOCH}_2\text{CH}_2\text{OH})$ through the replacement of the two water molecules in zinc formate by one ethylene glycol molecule. At ~100°C, the $\text{Zn}(\text{HCOO})_2(\text{HOCH}_2\text{CH}_2\text{OH})$ solvate dissolves in ethylene glycol to yield a colorless homogeneous solution, from which filamentous crystals of zinc formate glycoxide, $\text{Zn}(\text{HCOO})(\text{OCH}_2\text{CH}_2\text{O})_{1/2}$ or $\text{Zn}_2(\text{HCOO})_2(\text{OCH}_2\text{CH}_2\text{O})$, precipitate. At 150°C and above, the replacement of the formate ion in $\text{Zn}(\text{HCOO})(\text{OCH}_2\text{CH}_2\text{O})_{1/2}$ followed by the removal of this ion as formic acid from the solution yields the totally substituted zinc glycoxide $\text{Zn}(\text{OCH}_2\text{CH}_2\text{O})$, whose crystals have the shape of a distorted octahedron. Therefore, the major factor determining the degree of substitution of the formate ion in $\text{Zn}(\text{HCOO})_2 \cdot 2\text{H}_2\text{O}$ is the reaction temperature. Reaction (3) is completely reversible because, when $\text{Zn}(\text{HCOO})_2(\text{HOCH}_2\text{CH}_2\text{OH})$ is in contact with water vapor at room temperature, water replaces ethylene glycol in the solvate to yield $\text{Zn}(\text{HCOO})_2 \cdot 2\text{H}_2\text{O}$. A similar situation is observed in the water vapor hydrolysis of $\text{MC}_2\text{O}_4(\text{HOCH}_2\text{CH}_2\text{OH})$ solvates ($\text{M} = \text{Mn, Fe, Co, Zn}$) obtained by heating ethylene glycol + $\text{MC}_2\text{O}_4 \cdot 2\text{H}_2\text{O}$ mixtures [20–22]. In this case, raising the synthesis temperature does not lead to the formation of the partially or totally substituted glycoxide complex; that is, the process ends in the formation of the $\text{MC}_2\text{O}_4(\text{HOCH}_2\text{CH}_2\text{OH})$ solvate.

Depending on the reaction conditions and x , the $\text{Zn}_{1-x}\text{Co}_x(\text{HCOO})(\text{OCH}_2\text{CH}_2\text{O})_{1/2}$ solid solutions can be obtained both as filaments with a large length-to-diameter ratio and as long rods. Slowly heating a mixture of zinc and cobalt formates with ethylene glycol to 100–120°C followed by holding the mixture at this temperature for a certain time yields extended crystals of a solid solution:



The thinnest needle-like crystals of $\text{Zn}_{1-x}\text{Co}_x(\text{HCOO})(\text{OCH}_2\text{CH}_2\text{O})_{1/2}$ ($x = 0.05$) precipitate from the solution as it is evaporated slowly. The filamentous $\text{Zn}_{1-x}\text{Co}_x(\text{HCOO})(\text{OCH}_2\text{CH}_2\text{O})_{1/2}$ ($0.1 \leq x \leq 0.3$) crystals resulting from the first step of the process tend to longitudinal intergrowth, which results in the formation of intergrowths with a diameter of 0.5 μm and above. As x is increased, the $\text{Zn}_{1-x}\text{Co}_x(\text{HCOO})(\text{OCH}_2\text{CH}_2\text{O})_{1/2}$ crystals become shorter and their diameter increases to become 0.5 μm at $x = 0.3$. The partial replacement of zinc with cobalt in the $\text{Zn}_{1-x}\text{Co}_x(\text{HCOO})(\text{OCH}_2\text{CH}_2\text{O})_{1/2}$ structure imparts color to the crystals. As x is increased, the color density increases from light pink ($x = 0.005$) to intense lilac ($x = 0.3$). As the synthesis temperature is raised to 180°C, the filamentous lilac phase of $\text{Zn}_{1-x}\text{Co}_x(\text{HCOO})(\text{OCH}_2\text{CH}_2\text{O})_{1/2}$ gradually disappears, giving way to intensely blue crystals of the $\text{Zn}_{1-x}\text{Co}_x(\text{OCH}_2\text{CH}_2\text{O})$ solid solution. In outline, the formation of the cobalt-substituted glycooxide and cobalt glycooxide upon heating the formate + ethylene glycol mixture can be described by the following overall reactions:



Cobalt glycooxide crystallizes as very thin, optically near-isotropic flakes 0.5–1 μm in diameter and ~100 nm in thickness. The color of the powder is light violet. Chakroune et al. [23] synthesized cobalt glycooxide $\text{Co}(\text{OCH}_2\text{CH}_2\text{O})$ as discs by reacting cobalt acetate with ethylene glycol and determined its unit cell parameters to be $a = 3.09$ Å and $c = 8.27$ Å. In polarized light, the crystals of the solvate $\text{Zn}(\text{HCOO})_2(\text{HOCH}_2\text{CH}_2\text{OH})$ are colorless and appear as rhombic plates with low birefringence and refractive indexes of $Ng = 1.519$ and $Np = 1.492$. For comparison, $\text{Zn}(\text{HCOO})_2 \cdot 2\text{H}_2\text{O}$ has $Ng = 1.546$, $Nm = 1.519$, and $Np = 1.506$. Zinc formate

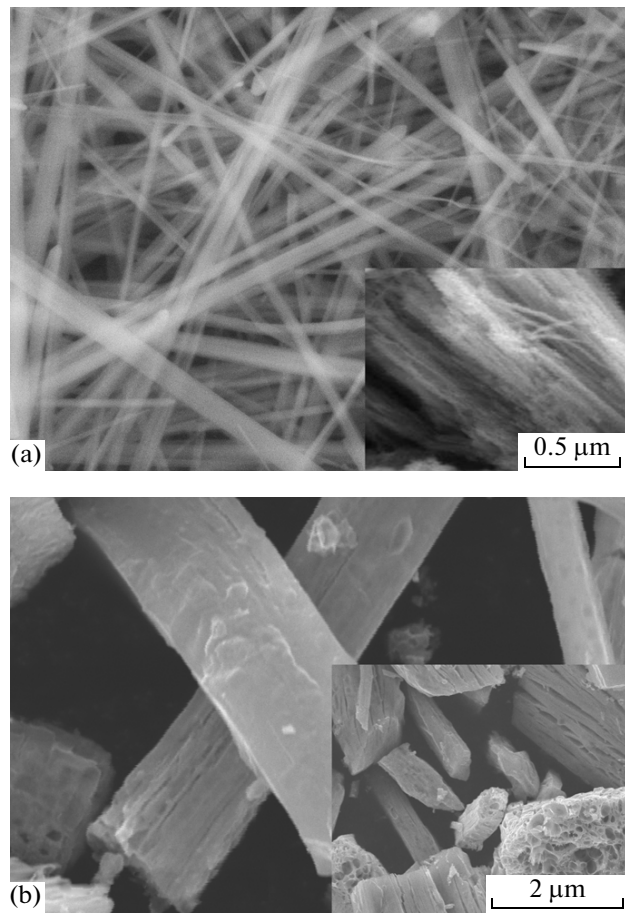


Fig. 1. SEM images of the $\text{Zn}(\text{HCOO})(\text{OCH}_2\text{CH}_2\text{O})_{1/2}$ (a) filaments and (b) bars and (insets) the products of their thermolysis at 450°C in air.

glycooxide $\text{Zn}(\text{HCOO})(\text{OCH}_2\text{CH}_2\text{O})_{1/2}$ crystallizes as thin colorless, needles. The crystals are very hygroscopic and are characterized by extinction parallel to their length. It seems impossible to determine the refractive indexes of filamentous $\text{Zn}(\text{HCOO})(\text{OCH}_2\text{CH}_2\text{O})_{1/2}$ because of its high hygroscopicity. As a supersaturated solution of $\text{Zn}(\text{HCOO})(\text{OCH}_2\text{CH}_2\text{O})_{1/2}$ is heated rapidly in ethylene glycol, the zinc salt can crystallize as bars, some of which having a diameter of about 2 μm. This allowed us to measure the refractive indexes of this compound with a sufficient degree of accuracy: $Ng = 1.609$, $Np = 1.543$, $\Delta(Ng - Np) = 0.066$. The morphology and size of the filamentous and barlike crystals of $\text{Zn}(\text{HCOO})(\text{OCH}_2\text{CH}_2\text{O})_{1/2}$ before and after their heat treatment are shown in Fig. 1. The filamentous crystals aggregate by forming longitudinal intergrowths (Fig. 1a). Upon heat treatment, the filamentous shape of the precursor crystals is inherited by the resulting zinc oxide particles. Similar transformations are observed for the barlike crystals of $\text{Zn}(\text{HCOO})(\text{OCH}_2\text{CH}_2\text{O})_{1/2}$, whose thermolysis product (ZnO) consists of barlike particles. These particles are porous or spongy and have a specific surface

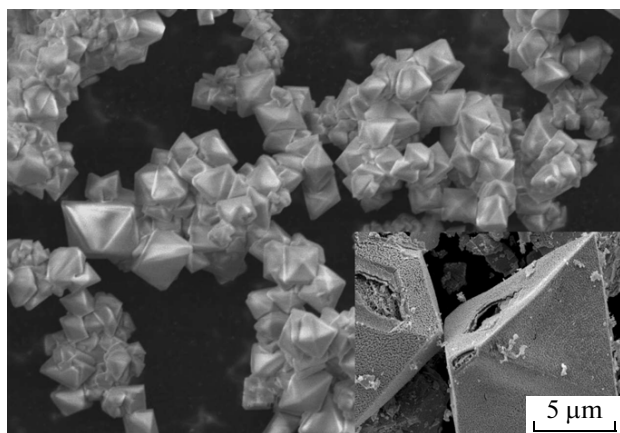


Fig. 2. SEM images of $\text{Zn}_{0.9}\text{Co}_{0.1}(\text{OCH}_2\text{CH}_2\text{O})$ crystals and (inset) the products of their thermolysis at 450°C in air.

area of $23.5 \text{ m}^2/\text{g}$. Zinc glycoxide $\text{Zn}(\text{OCH}_2\text{CH}_2\text{O})$ forms colorless crystals as distorted octahedra with very imperfect cleavages. The refractive indexes of its single crystals are $N_g = 1.581$, $N_m = 1.564$, $N_p = 1.548$, and $\Delta(N_g - N_p) = 0.033$. The substitution of cobalt for zinc raises the maximum refractive index and birefringence; for example, for $\text{Zn}_{0.95}\text{Co}_{0.05}(\text{OCH}_2\text{CH}_2\text{O})$: $N_g = 1.585$, $N_m = 1.567$, $N_p = 1.546$, and $\Delta(N_g - N_p) = 0.039$. Note that increasing the cobalt content of the

$\text{Zn}_{1-x}\text{Co}_x(\text{OCH}_2\text{CH}_2\text{O})$ solid solution does not exert any significant effect on the position of the reflections in its X-ray diffraction pattern. This pseudomorphic transformation into the oxide phase is also typical of $\text{Zn}_{1-x}\text{Co}_x(\text{OCH}_2\text{CH}_2\text{O})$ with $0 \leq x \leq 0.3$. Figure 2 shows the SEM images of $\text{Zn}_{0.9}\text{Co}_{0.1}(\text{OCH}_2\text{CH}_2\text{O})$ crystals and the product of their thermolysis at 450°C (inset). In this case, the pseudocrystals of the thermolysis product are built of minute zinc oxide grains and have a large number of cavities. The specific surface area of $\text{Zn}_{1-x}\text{Co}_x\text{O}$ ($0 \leq x \leq 0.3$) is $32 \text{ m}^2/\text{g}$.

The thermal decomposition of filamentous $\text{Zn}(\text{HCOO})(\text{OCH}_2\text{CH}_2\text{O})_{1/2}$ and $\text{Zn}_{1-x}\text{Co}_x(\text{HCOO})(\text{OCH}_2\text{CH}_2\text{O})_{1/2}$ ($0 < x \leq 0.2$) in air occurs exothermically in two steps at ~ 300 – 390 and 400 – 480°C (Fig. 3a). The weight loss for $\text{Zn}(\text{HCOO})(\text{OCH}_2\text{CH}_2\text{O})_{1/2}$ at 450°C is 41.5 wt \% , approximately 0.5 wt \% less than is expected for the decomposition of this compound to ZnO (42.03 wt \%). For the thermolysis of the $\text{Zn}_{1-x}\text{Co}_x(\text{HCOO})(\text{OCH}_2\text{CH}_2\text{O})_{1/2}$ solid solutions, the actual weight loss differs from the expected weight loss by an average of 0.65 wt \% . The observed discrepancy between the theoretical and experimental weight loss values is due to the presence of bound carbon in the samples, whose content is 0.53 – 0.76 wt \% for $0 \leq x \leq 0.1$, according to elemental analysis data. The thermolysis of the $\text{Zn}_{1-x}\text{Co}_x(\text{OCH}_2\text{CH}_2\text{O})$ ($0 \leq x \leq 0.2$) glycoxides occurs exothermically in a single step (Fig. 3b). The weight loss for $\text{Zn}(\text{OCH}_2\text{CH}_2\text{O})$ at 450°C is 34.6 wt \% ,

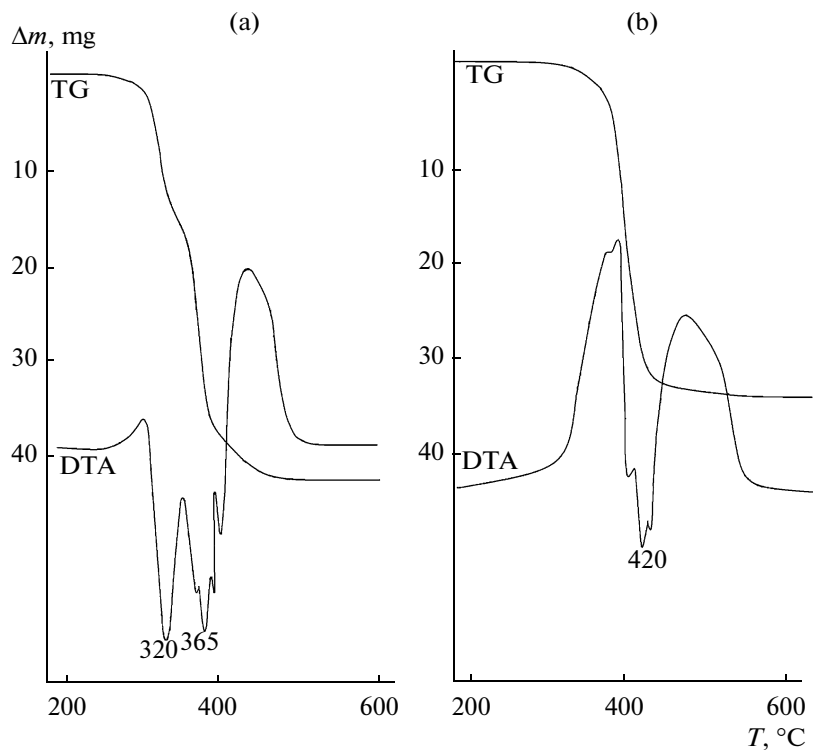


Fig. 3. TG and DTA profiles for (a) $\text{Zn}(\text{HCOO})(\text{OCH}_2\text{CH}_2\text{O})_{1/2}$ and (b) $\text{Zn}(\text{OCH}_2\text{CH}_2\text{O})$.

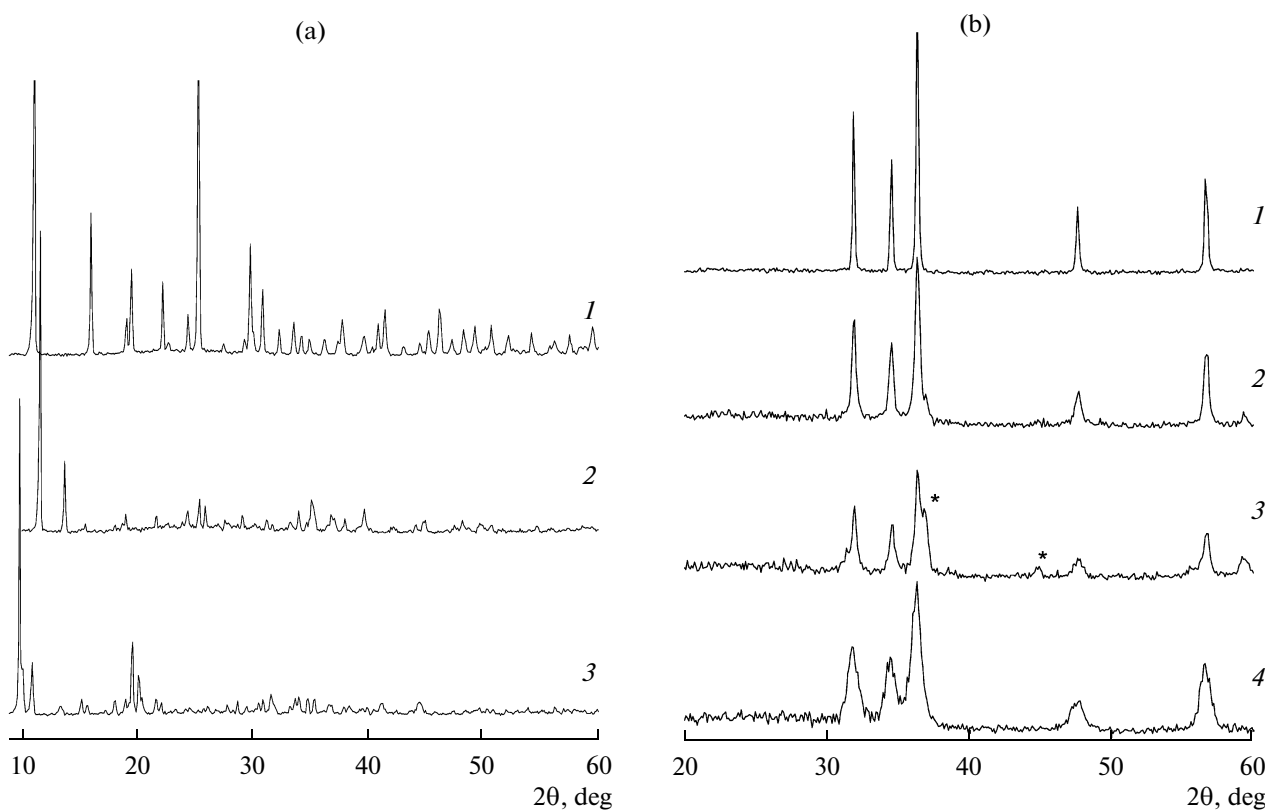


Fig. 4. (a) X-ray diffraction patterns of (1) $\text{Zn}(\text{HCOO})_2(\text{HOCH}_2\text{CH}_2\text{OH})$, (2) $\text{Zn}(\text{HCOO})(\text{OCH}_2\text{CH}_2\text{O})_{1/2}$, and (3) $\text{Zn}(\text{OCH}_2\text{CH}_2\text{O})$; (b) those of the products of the thermolysis of $\text{Zn}_{1-x}\text{Co}_x(\text{HCOO})(\text{OCH}_2\text{CH}_2\text{O})_{1/2}$ in (1–3) air ($x = (1) 0.05$, (2) 0.2, and (3) 0.3) and (4) helium ($x = 0.2$) at 450°C . The reflections from the minor phase with a cubic spinel structure are starred.

which is 0.5 wt % below the value expected for the complete decomposition of the compound to zinc oxide (35.1 wt %). Again, elemental analysis data indicate the incomplete removal of carbon from all $\text{Zn}_{1-x}\text{Co}_x\text{O}$ solid solutions obtained at 450°C . For the glycoxide complexes heat-treated in a helium atmosphere, the thermolysis product has a higher carbon content of 2–5 wt %, depending on the nature of the complex. While the product of $\text{Zn}_{0.95}\text{Co}_{0.05}(\text{HCOO})(\text{HOCH}_2\text{CH}_2\text{O})_{1/2}$ thermolysis in the inert gas medium contains 2.1 wt % carbon, the carbon content of the $\text{Zn}_{0.95}\text{Co}_{0.05}(\text{OCH}_2\text{CH}_2\text{O})$ thermolysis product is 4.62 wt %. Note that the weight loss of the samples heated in air to 750°C at a rate of 10 K/min is nearly equal to the value expected for the formation of ZnO or $\text{Zn}_{1-x}\text{Co}_x\text{O}$. Based on the results of the thermogravimetric and elemental analyses, the composition of the glycoxide thermolysis products can be represented as $\text{Zn}_{1-x}\text{Co}_x\text{O}_{1-y}\text{C}_y$.

Figure 4 presents the X-ray diffraction patterns of the solvate $\text{Zn}(\text{HCOO})_2(\text{HOCH}_2\text{CH}_2\text{OH})$, zinc formate glycoxide $\text{Zn}(\text{HCOO})(\text{OCH}_2\text{CH}_2\text{O})_{1/2}$, zinc glycoxide $\text{Zn}(\text{OCH}_2\text{CH}_2\text{O})$, and the products of the thermolysis of $\text{Zn}_{1-x}\text{Co}_x(\text{HCOO})(\text{OCH}_2\text{CH}_2\text{O})_{1/2}$ in air ($x = 0.2, 0.3$) and in helium ($x = 0.2$) at 450°C . The substitution of cobalt for zinc in these compounds

causes no significant changes in their diffraction patterns. The thermolysis product of $\text{Zn}_{1-x}\text{Co}_x(\text{HCOO})(\text{OCH}_2\text{CH}_2\text{O})_{1/2}$ with $x = 0.3$ contains $\text{Zn}_{1-x}\text{Co}_x\text{O}$ with a wurtzite structure as the major phase and a minor amount of a cubic spinel, probably $\text{Co}_{3-y}\text{Zn}_y\text{O}_4$. According to X-ray diffraction data, the latter phase is present in the thermolysis products of the $x > 0.20$ glycoxides. As was demonstrated by transmitted polarized light microscopy, the samples heat-treated in the inert atmosphere consist of black, nontransparent objects pseudomorphic to the crystals of the precursor—zinc formate glycoxide or zinc glycoxide. The black color of the pseudocrystals is due to the presence of elemental carbon. The carbon is almost entirely removed as the sample is heat-treated in air at 450°C , and the sample turns greenish.

The IR spectrum of $\text{Zn}(\text{HCOO})(\text{OCH}_2\text{CH}_2\text{O})_{1/2}$ (Fig. 5) can be viewed as the superposition of the spectra of the HCOO^- and $\text{OCH}_2\text{CH}_2\text{O}^{2-}$ anions. The very strong absorption band at 1574 cm^{-1} and the strong band at 1361 cm^{-1} are due to the asymmetric and symmetric vibrations of the carboxyl group (COO) of the formate ion [24]. The C—O bond vibrations in the $\text{OCH}_2\text{CH}_2\text{O}^{2-}$ ion coordinated to zinc give rise to two very strong bands at 1084 and 1043 cm^{-1} , which are close to the corresponding IR bands of liquid ethylene

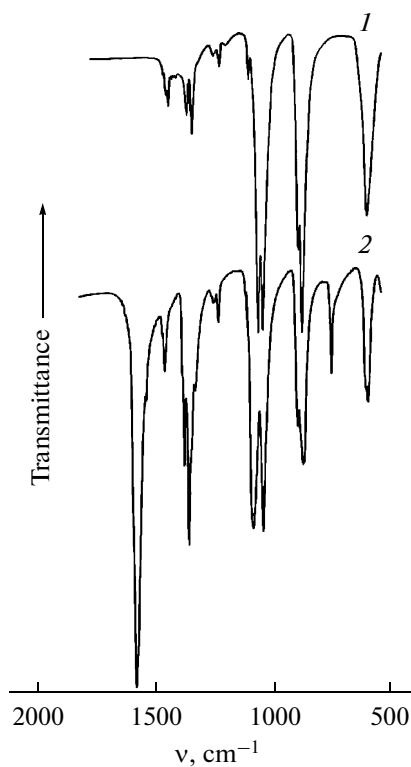


Fig. 5. IR spectra of (1) $\text{Zn}(\text{OCH}_2\text{CH}_2\text{O})$ and (2) $\text{Zn}(\text{HCOO})(\text{OCH}_2\text{CH}_2\text{O})_{1/2}$.

glycol (1087 and 1043 cm^{-1}) [25], vanadyl glycoxide $\text{VO}(\text{OCH}_2\text{CH}_2\text{O})$ (1060 and 1012 cm^{-1}), and titanium glycoxide $\text{Ti}(\text{OCH}_2\text{CH}_2\text{O})_2$ (1055 and 1033 cm^{-1}) [18]. The twisting vibrations of the C–C bonds show themselves as very strong absorption bands at 899 and 871 cm^{-1} , which are shifted to higher frequencies relative to the same bands of liquid ethylene glycol (883 and 862 cm^{-1}) and to lower frequencies relative to the corresponding bands of vanadyl glycoxide (925 and 887 cm^{-1}) and titanium glycoxide (916 and 878 cm^{-1}). The IR spectrum of $\text{Zn}(\text{OCH}_2\text{CH}_2\text{O})$ differs markedly from that of $\text{Zn}(\text{HCOO})(\text{OCH}_2\text{CH}_2\text{O})_{1/2}$ (Fig. 5): all of its bands can be assigned with confidence to vibrations of the $\text{OCH}_2\text{CH}_2\text{O}^{2-}$ ion and Zn–O bonds. The absorption bands of the C–O bonds (1068 and 1049 cm^{-1}) are strongly shifted toward one another as compared to the corresponding bands in the IR spectra of liquid ethylene glycol and $\text{Zn}(\text{HCOO})(\text{OCH}_2\text{CH}_2\text{O})_{1/2}$. At the same time, the frequencies of the twisting vibrations of the C–C bonds are increased to 898 and 881 cm^{-1} . The substitution of cobalt for zinc yielding $\text{Zn}_{1-x}\text{Co}_x(\text{HCOO})(\text{OCH}_2\text{CH}_2\text{O})_{1/2}$ or $\text{Zn}_{1-x}\text{Co}_x(\text{OCH}_2\text{CH}_2\text{O})$ solid solutions causes no noticeable changes in the IR spectra.

For estimating the photocatalytic efficiency of the wurtzite-type $\text{Zn}_{1-x}\text{Co}_x\text{O}$ solid solutions obtained by $\text{Zn}_{1-x}\text{Co}_x(\text{HCOO})(\text{OCH}_2\text{CH}_2\text{O})_{1/2}$ and $\text{Zn}_{1-x}\text{Co}_x(\text{OCH}_2\text{CH}_2\text{O})$ ($0 \leq x \leq 0.3$) thermolysis, we studied their effect on the decomposition rate

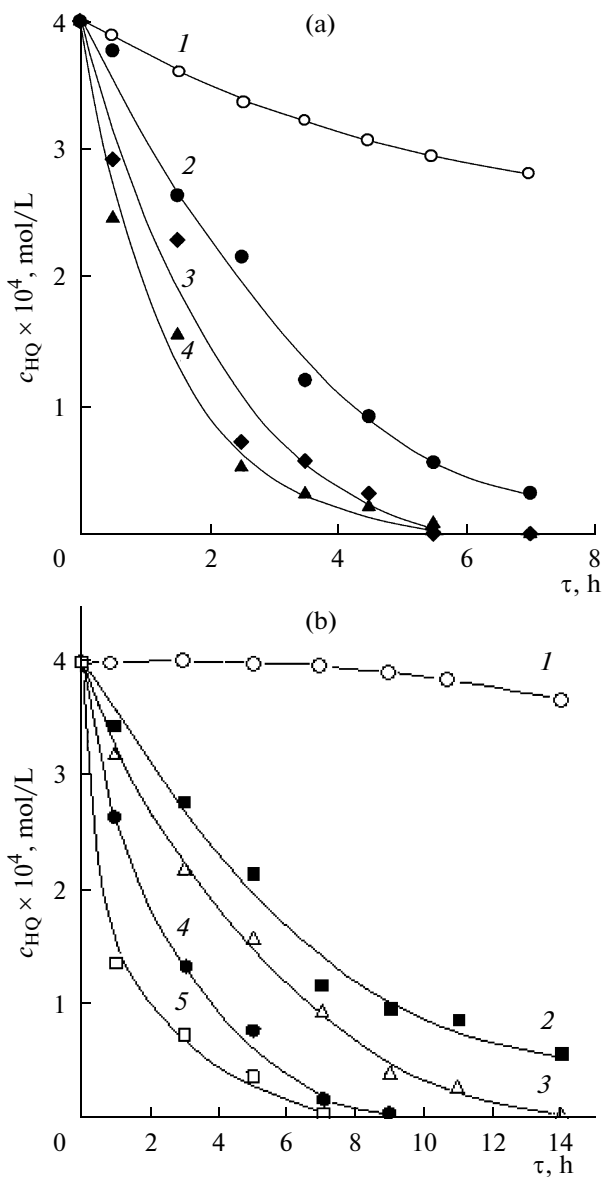


Fig. 6. Hydroquinone (HQ) concentration as a function of time: (a) UV irradiation of the solution (1) in the absence of a catalyst and (2–4) in the presence of (2) ZnO whiskers, (3) $\text{Zn}_{0.8}\text{Co}_{0.2}\text{O}$ whiskers, and (4) $\text{Zn}_{0.8}\text{Co}_{0.2}\text{O}$ pseudocrystals. (b) The same for blue light-irradiated solution (1) in the absence of a catalyst and (2–5) in the presence of whiskers of (2) $\text{Zn}_{0.99}\text{Co}_{0.01}\text{O}$, (3) $\text{Zn}_{0.95}\text{Co}_{0.05}\text{O}$, (4) $\text{Zn}_{0.8}\text{Co}_{0.2}\text{O}$, and (5) $\text{Zn}_{0.7}\text{Co}_{0.3}\text{O}$.

of a standard organic compound in water under UV irradiation. The organic standard was hydroquinone, which is among the strongest organic toxicants in natural water. Catalyst samples were prepared by heating the precursors to 450°C at a rate of 10 K/min and holding them at this temperature for 2 h. (These heating conditions were found to be optimal.) These experiments demonstrated that, for all $\text{Zn}_{1-x}\text{Co}_x\text{O}$ solid solutions, the rate of hydroquinone oxidation

under UV irradiation ($\lambda_{\max} = 253$ nm) increases definitely with an increasing cobalt content. The highest photocatalytic activity is shown by $Zn_{0.7}Co_{0.3}O$, which contains a minor amount of a cubic spinel phase, probably $Co_{3-y}Zn_yO_4$. These experimental data are in agreement with the high photocatalytic performance of Co_3O_4 in methyl orange oxidation [26]. The slightly higher catalytic activity of the pseudocrystalline versus quasi-1D $Zn_{1-x}Co_xO$ samples at the early stages of the process is likely due to the difference between their specific surface areas ($32\text{ m}^2/\text{g}$ for the former against $25\text{ m}^2/\text{g}$ for the latter). These catalytic activity data are presented in Fig. 6a, which shows how the hydroquinone concentration in the solution varies with time under UV irradiation in the absence of a catalyst and in the presence of ZnO , $Zn_{0.8}Co_{0.2}O$, and pseudocrystals of $Zn_{0.8}Co_{0.2}O$. The photocatalytic activity of $Zn_{1-x}Co_xO$ in blue light depends on the cobalt content of the catalyst in a similar way. Figure 6b demonstrates how the hydroquinone concentration in the solution varies with time in blue light in the absence of a catalyst and in the presence of $Zn_{1-x}Co_xO$ ($x = 0.01, 0.05, 0.2, 0.3$) whiskers. It is impossible to determine the effect of bound carbon on the photocatalytic properties of $Zn_{1-x}Co_xO$ and $Zn_{1-x}Co_xO_{1-y}C_y$ because the carbon contents of the samples are nearly equal. However, it was reported that the photocatalytic activity of pure zinc oxide can be enhanced by introducing carbon [27]. Therefore, the residual carbon staying in the oxide after the thermolysis of the glycoxide precursor at least does not exert an adverse effect on the catalyst.

Thus, we have devised and carried out the targeted synthesis of micron- and nanometer-sized $Zn_{1-x}Co_xO$ ($0 \leq x \leq 0.2$) solid solutions and heterogeneous materials with $x > 0.2$ in two morphological types. These materials are promising catalysts for the photocatalytic oxidation of hydroquinone in UV and blue light. A correlation has been established between the photocatalytic activity of $Zn_{1-x}Co_xO$ and x . The photocatalytic activity of the catalysts depends more strongly on x than on their particle size or specific surface area.

ACKNOWLEDGMENTS

This study was supported by the Russian Foundation for Basic Research, project no. 09-03-00252-a.

REFERENCES

- X. Q. Meng, D. Z. Shen, J. Y. Zhang, et al., Solid State Commun. **135**, 179 (2005).
- J. Xie, P. Li, W. Yanji, and Y. Wei, J. Phys. Chem. Solids **70**, 112 (2009).
- Y. Wang and M. Li, Mater. Lett. **60**, 266 (2006).
- J. Xie, P. Li, W. Yanji, and Y. Wei, Phys. Status Solidi A **205**, 1560 (2008).
- M. Yang, G. Pang, L. Jiang, and S. Feng, Nanotechnol. **17**, 206 (2006).
- Q. Ahsanulhaq, J.-H. Kim, and Y.-B. Hahn, Nanotechnol. **18** (485307) (2007).
- K. Byrappa, A. K. Subramani, S. Ananda, et al., Bull. Mater. Sci. **29**, 433 (2006).
- X. Ren, D. Han, D. Chen, and F. Tang, Mater. Res. Bull. **42**, 807 (2007).
- A. J. Attia, S. H. Kadhim, and F. H. Hussein, E.-J. Chem. **5**, 219 (2008).
- J. Zheng, Z.-Y. Jiang, Q. Kuang, et al., J. Solid State Chem. **182**, 115 (2009).
- A. C. Dodd, A. J. McKinley, M. Saunders, and T. Tzusuki, Microsc. Microanal. **11**, 500 (2005).
- S. Ekambaram, Y. Iikubo, and A. Kudo, J. Alloys Compd. **433**, 237 (2007).
- Q. Xiao, J. Zhang, C. Xiao, and X. Tan, Mater. Sci. Eng. (B) **142**, 121 (2007).
- L. Chen, J. Zhang, X. Zhang, et al., Optics Express **16**, 11795 (2008).
- C. J. Cong, J. H. Hong, and K. L. Zhang, Mater. Chem. Phys. **113**, 435 (2009).
- X. Jian, Y. Wang, T. Herricks, and Y. Xia, J. Mater. Chem. **14**, 695 (2004).
- D. Wang, R. Yu, Y. Chen, et al., Solid State Ionics **172**, 101 (2004).
- V. N. Krasil'nikov, A. P. Shtin, O. I. Gyrdasova, et al., Ros. Nanotekhnol. **3**, 107 (2008).
- O. I. Gyrdasova, V. N. Krasil'nikov, G. V. Bazuev, et al., *Proceedings of the 11th International Symposium "Order, Disorder, and Properties of Oxides"* (pos. Loo, Rostov-on-Don, Russia) [in Russian], Vol. 1, p. 128.
- O. I. Gyrdasova, V. N. Krasil'nikov, I. G. Grigorov, and G. V. Bazuev, Zh. Neorg. Khim. **51**, 1020 (2006).
- V. N. Krasil'nikov, O. I. Gyrdasova, and G. V. Bazuev, Zh. Neorg. Khim. **53**, 1984 (2006).
- V. N. Krasil'nikov, O. I. Gyrdasova, and G. V. Bazuev, Zh. Neorg. Khim. **54**, 1097 (2008).
- N. Chakroune, G. Viau, S. Ammar, et al., New J. Chem. **29**, 355 (2005).
- K. Nakamoto, *Infrared and Raman Spectra of Inorganic and Coordination Compounds* (Wiley, New York, 1986; Mir, Moscow, 1991).
- H. Matsuura and T. Miyazawa, Bull. Chem. Soc. Jpn. **40**, 85 (1967).
- Y. Chen, L. Hu, M. Wang, et al., Colloids Surf. **336**, 64 (2009).
- K. Byrappa, A. K. Subramani, S. Ananda, et al., J. Mater. Sci. **41**, 1355 (2006).